

We are IntechOpen, the world's leading publisher of Open Access books Built by scientists, for scientists

6,900

Open access books available

186,000

International authors and editors

200M

Downloads

Our authors are among the

154

Countries delivered to

TOP 1%

most cited scientists

12.2%

Contributors from top 500 universities



WEB OF SCIENCE™

Selection of our books indexed in the Book Citation Index
in Web of Science™ Core Collection (BKCI)

Interested in publishing with us?
Contact book.department@intechopen.com

Numbers displayed above are based on latest data collected.
For more information visit www.intechopen.com



Clinical Usefulness of Contrast-Enhanced Three-Dimensional Ultrasound Imaging with Sonazoid for Hepatic Tumor Lesions

Kazushi Numata¹, Wen Luo^{1,2}, Manabu Morimoto¹,
Hiroyuki Fukuda¹, Naoto Sato³ and Katsuaki Tanaka¹

¹*Gastroenterological Center, Yokohama City University Medical Center,
4-57 Urafune-cho, Minami-ku, Yokohama, Kanagawa, 232-0024,*

²*Department of Ultrasound, Xijing Hospital, Fourth Military Medical University,
15th Changle Xi Road, Xi'an, Shaanxi, 710032,*

³*GE Healthcare Japan Corporation, 4-7-127, Asahigaoka, Hino, Tokyo 191-8503*

^{1,3}*Japan*

²*China*

1. Introduction

In the last few years, three-dimensional ultrasound (3D US) imaging has attracted the interest among medical imaging researchers, because of its unique ability to provide images in three orthogonal planes, and the imaging tool has been proven to be useful clinically in the fields of obstetrics, hepatology, cardiology, urology, and mastology (Badea et al., 2007; Benacerraf et al., 2006; Tutschek & Sahn, 2007; Taylor et al., 2005; Kotsianos-Hermle et al., 2009).

Multiplanar 3D US imaging is thought to provide more spatial information and allow easier anatomic assessment than the conventional two-dimensional ultrasound imaging. Contrast-enhanced three-dimensional ultrasound (CE 3D US) imaging is a new medical imaging technique that uses reflections of microbubbles to clearly depict blood vessels and allows the images to be displayed spatially at different visual angles. Although CE 3D US imaging has recently been evaluated as a tool for clinical diagnosis (Krenning et al., 2007; Yukisawa et al., 2007; Ohto et al., 2005; Wessels et al., 2004; Forsberg et al., 2004), only a few studies have investigated its usefulness in the assessment of hepatic tumors (Yukisawa et al., 2007; Ohto et al., 2005). Hepatic tumors, especially hepatocellular carcinoma (HCC), remain one of the most commonly encountered diseases worldwide (Bosch et al., 2004), and efficacious methods for the diagnosis and therapy of this disease, including CE 3D US imaging, need to be explored further (Camaggi et al., 2007; Kudo, 2007; Dietrich, 2002).

Sonazoid (Daiichi Sankyo, Tokyo, Japan) is a newly-developed second-generation ultrasound contrast agent that has been used clinically in Japan since January 2007 for the evaluation of liver tumors and for phase-inversion harmonic gray-scale sonography. Sonazoid consists of perfluorobutane surrounded by a phospholipid shell and has been reported, from previous studies, to be stable enough to allow image acquisition under ultrasound exposure for 5 to 10 minutes (Numata et al., 2008; Halpern et al., 2002).

Currently, automatically scanned CE 3D US with Sonazoid using the GE LOGIQ 7 ultrasound system (GE Healthcare, Milwaukee, WI, USA) is being used as a clinical diagnostic tool in Japan, especially for liver lesions (Luo et al., 2009a; Luo et al., 2009b; Luo et al., 2009c; Luo et al., 2010a; Luo et al., 2010b; Numata et al., 2010a; Numata et al., 2010b). With the use of coded harmonic angio (CHA) mode and high mechanical index (MI) contrast conditions, which reduce microbubbles in microvessels, but not in relatively large vessels, such as tumor vessels and portal veins, CE 3D US with Sonazoid facilitates detailed observation of tumor vessels. As compared to CE (two dimensional) US with Sonazoid, automatically scanned CE 3D US with Sonazoid allows the volume of interest to be viewed in three orthogonal planes, thereby more spatial information and facilitating easier anatomic assessment.

In this chapter, we present the methods used for acquisition and reconstruction of CE 3D US images obtained with Sonazoid, and also clinical usefulness of this diagnostic modality in the evaluation of hepatic tumor lesions, especially HCC lesions, using many figures to facilitate comprehension.

2. US equipment

The US scanning was performed with a commercially available ultrasound imaging system (LOGIQ 7; GE Healthcare, Milwaukee, WI) and a convex volume 4D3C-L probe with a frequency of 2.0-5.5 MHz.

3. Advantage of Sonazoid over Levovist as a contrast agent for CE 3D US

In our experience, Levovist is unstable, and therefore, not a suitable contrast agent for CE 3D US. As with Levovist, contrast-enhanced US with Sonazoid involves two phases of contrast enhancement: the vascular phase and the late (parenchyma-specific, delayed, post-vascular) phase. The drawback of the poor stability of Levovist is overcome with the high stability of Sonazoid and the microbubbles of Sonazoid have the advantage of allowing more prolonged imaging and providing stronger contrast effects; hence, more detailed observations are possible with Sonazoid than with Levovist.

4. CE 3D US at a high mechanical index (MI)

Sonazoid-enhanced US at a low MI using software for a low MI contrast mode (coded phase inversion mode: CPI mode) permits visualization of tumor vessels and tumor enhancement of liver lesions. However, not only relatively large vessels, such as tumor vessels and portal veins, but also microvessels within the liver parenchyma become rapidly filled with Sonazoid microbubbles under low MI conditions, which in turn, permits rapid enhancement of the tumor and of the liver parenchyma simultaneously. This phenomenon allows only a short time for detailed observation of the tumor vessels and tumor enhancement in the vascular phase of Sonazoid-enhanced US.

Sonazoid-enhanced US at a high MI using software for a high MI contrast mode (coded harmonic angio mode: CHA mode) allows observation of vessels in the early phase by eliminating microbubbles in the microvessels but not in the relatively large vessels, such as tumor vessels and portal veins (Numata et al., 2008), which permits a more prolonged observation time of the tumor vessels, clear tumor enhancement, and also automatically scanned CE 3D US with Sonazoid.

5. Data acquisition

2D grey-scale US was carried out for identifying the tumor prior to the CE 3D US, and also for measurement of the tumor size.

Prior to the CE 3D US, 0.2 mL Sonazoid was injected as a bolus by hand through an antecubital vein, followed by injection of 2 mL of 5% glucose and then a infusion of glucose at 10 mL/min. The coded harmonic angio (CHA) mode with a mechanical index (MI, 0.5-0.9) of 8 to 13 frames per second was used for the CE US. The entire contrast procedure was divided into three phases: early phase, 15-50 s after injection of the contrast medium; middle phase, 80-120 s after injection of contrast medium; late phase, more than 5 minutes after injection of contrast medium.

For data acquisition, the ultrasound imaging system is equipped with two functions: the Static 3D function and the Autosweep 3D function. For both functions, the probe held by the sonographer automatically sweeps the region in the volume of interest (VOI), the size and position of which is already adjusted on the grey-scale US to contain the target tumor and the surrounding tissues. Static 3D enables easy volume scanning and rendering. However, it is difficult to control the complex acoustic power protocol required for high-MI contrast imaging, and this may cause unexpected bubble destructions in the middle and late phases. On the other hand, the AutoSweep 3D provides the acoustic power control needed for high-MI imaging, without unexpected bubble destructions. Therefore, in the early phase we performed two scanning procedures using the two functions, while in the two subsequent phases, only one procedure each was conducted, with the Autosweep 3D. The scanning angle can be selected in the range of 15° to 84°. We used angles in the range of 30°-70°, depending on the tumor size.

When we used the Static 3D for the data acquisition in the early phase, there were five levels of acquired image quality, Max, Hi 2, Hi 1, Mid 2, Mid 1, and Low. The Max level combined the highest density with the slowest speed, and the Low level combined the lowest density with the highest speed. Both the scanning time and image quality should be taken into consideration for proper image acquisition. The Mid 2 or Hi1 quality was selected for the patients, considering the short breath-holding duration. Accordingly, the time for one scanning session was 4.5 s to 26 s (mean 10 s). Therefore, the number of scanning sessions was 1 or 2 times during the early phase using the Static 3D function. The data acquired were stored as cineloops in the hard disk of the ultrasound imaging system.

When we used the Autosweep 3D for data acquisition in each of the three phases, there were four levels of acquired image quality, low, mid, high, and max. The mid quality was selected for the patients, considering the short breath-holding duration. Accordingly, the time for one scanning session was 3 s to 11 s (mean 6 s). The number of scanning sessions was 1 to 4 during the early phase, 1 to 2 during the middle phase, and 1 to 4 using the Autosweep 3D function. The data acquired were automatically stored as cineloops in the hard disk of the ultrasound imaging system. Subsequently, we selected the good data obtained in each phase for the image reconstruction.

6. Image reconstruction

3D image reconstruction was performed using the functions with which the LOGIQ 7 ultrasound system was equipped. In the VOI which was presented in an isotropic rectangular coordinate frame, the three orthogonal planes were referred to as plane A,

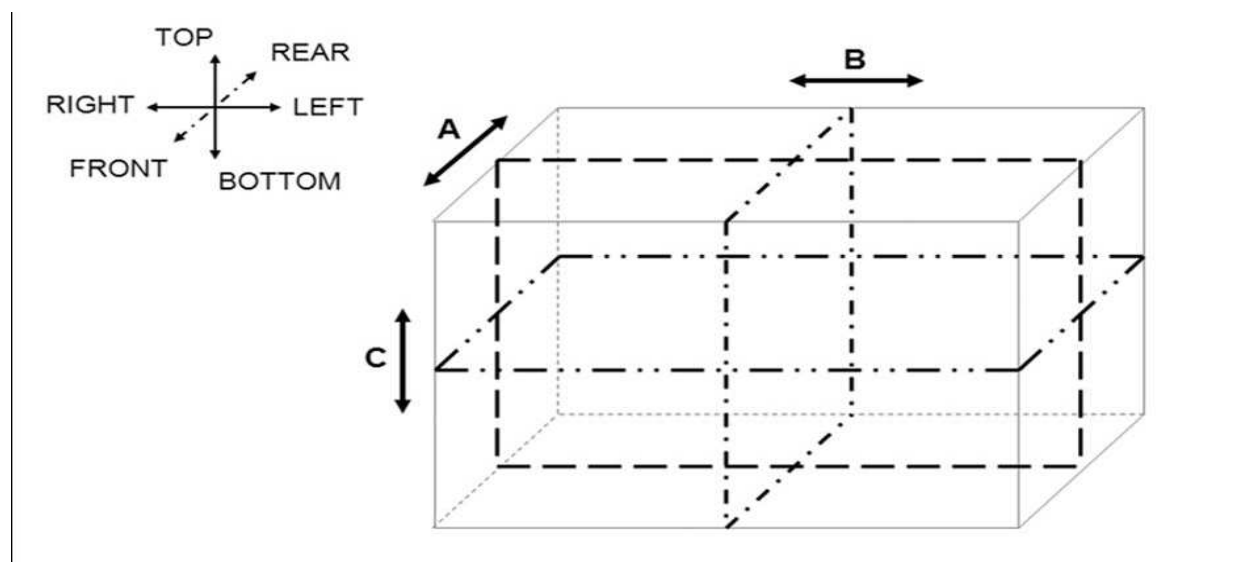


Fig. 1. Illustration of the volume of Interest and three orthogonal planes obtained by automatic 3D acquisition. Plane A moves from the front to the rear, or in the opposite direction, through the volume of interest, whereas plane B moves from the left to the right, or in the opposite direction, and plane C moves from the top to the bottom, or in the opposite direction.

which could migrate from the front to the rear through the VOI, plane B, which moved from the left to the right, and plane C, which moved from the top to the bottom (Fig. 1).

Tomographic ultrasound images (TUI) with presentation of several parallel slices in three orthogonal planes were reconstructed in three phases, while the number of slices that could be selected was 2, 4, or 6 for images obtained using the Autosweep 3D, and 2, 4, or 9 for the Static 3D. In order to show the desired images, the range of distance between two slices in the TUI could be adjusted as required (Figs. 2A-C). The mean time taken for these procedures was about 20 s.

Sonographic angiograms were reconstructed in an angio-like view during the early phase using various rendering modes. When the Autosweep 3D was used, the five rendering modes consisted of the surface mode, texture mode, and maximum intensity projection mode, average intensity mode, and minimum intensity modes, which could be used in any combination (Fig. 2D). The maximum intensity projection mode displaying the maximal gray values in the VOI, combined with the surface mode displaying the gray values on the surfaces of the anatomic structures, was used to visualize the tumor vessels and early tumor enhancement in the early phase. While the average intensity mode displaying the average gray values in the VOI was employed in combination with the surface mode, to define the tumor based on the predominantly unenhanced areas in the early, middle and late phases. The mean time taken for these procedures was about 45 s.

When the Static 3D was used for the reconstruction of the data obtained in the early phase, the transparent maximum mode (as same as the maximum intensity projection mode) combined with the surface smooth mode was selected to depict the tumor vessels and the tumor enhancement distinctly. The transparent X-ray mode (as same as the average intensity mode) combined with the surface smooth mode (as same as the surface mode) was used for detection of the unenhanced areas within the tumors, if these unenhanced portions played an important role in defining the tumors, such as unenhanced portions of metastases

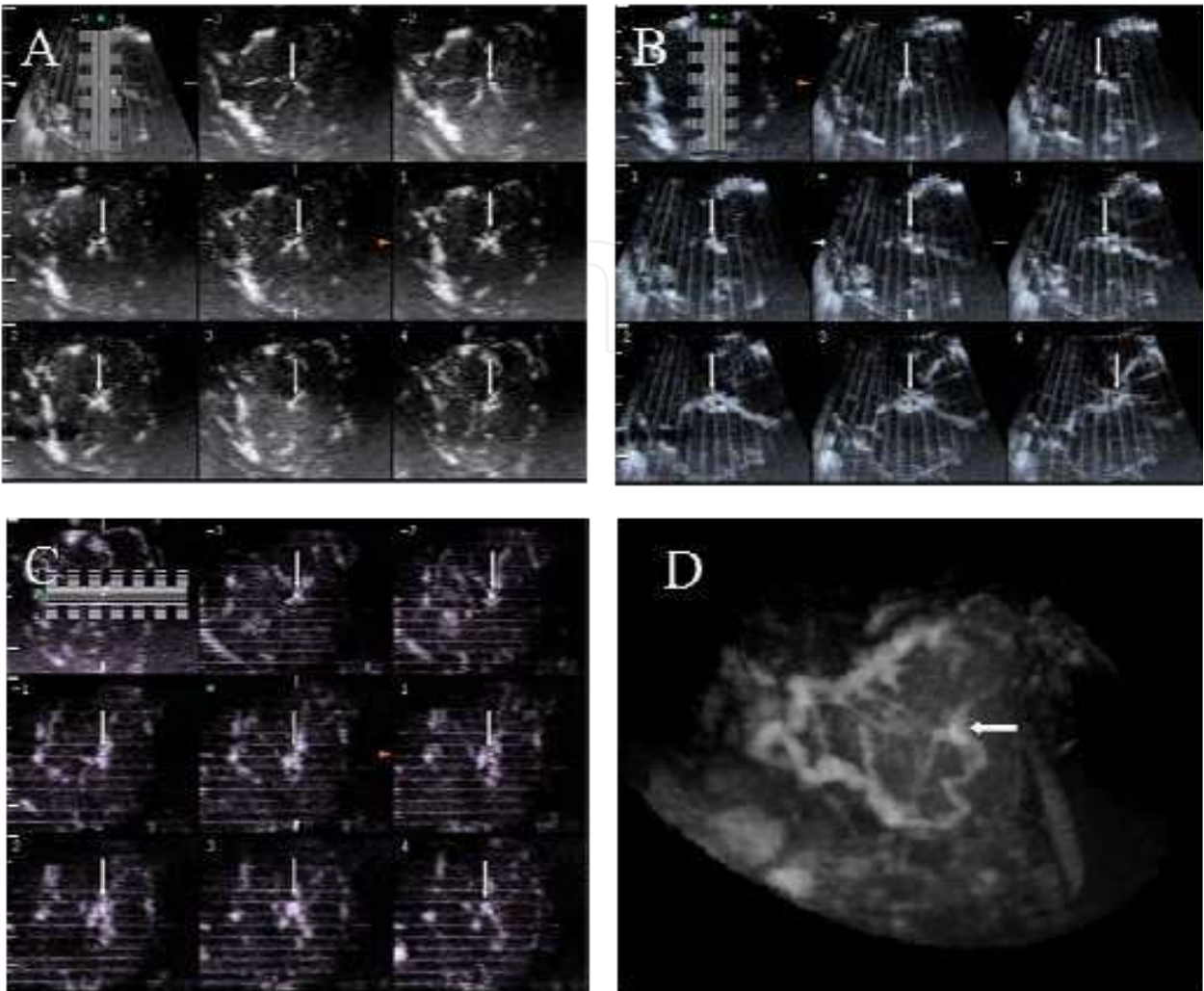


Fig. 2. Early-phase contrast-enhanced three-dimensional ultrasonographic (CE 3D US) images of the liver in a patient with focal nodular hyperplasia (maximum diameter, 50 mm) in the left lobe. A-C: Tomographic ultrasound images (TUI) in plane A, which could be translated from front to back (A), plane B, which could be translated from right to left (B), and plane C, which can be translated from bottom to top. The slice distance is 1.0 mm in each plane. Slight cardiac motion artifacts are seen in planes B and C. Sonographic angiograms acquired by CE 3D US with the Autosweep 3D in the early phase and rendered using the maximum intensity projection mode mixed with the surface mode; the images show the tumor to contain a spoke-wheel artery (D). Arrows indicate the spoke-wheel artery.

with early peripheral ring-like enhancement accounting for large areas of the tumors. In cases of hypervascular tumors, such as typical HCC lesions or focal nodular hyperplasia, the transparent maximum mode (maximum intensity projection mode) alone was selected to simplify the procedure to depict the intratumoral vessels with early tumor enhancement distinctly. Tortuous vessels within the lesion could be clearly visualized (Fig. 3). The mean time taken for these procedures was about 60 s.

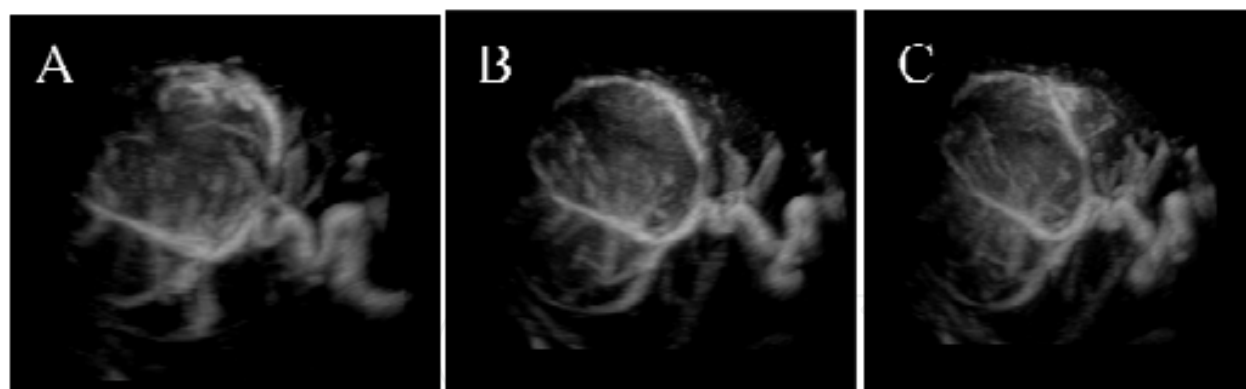


Fig. 3. Early-phase of CE 3D US images of the liver in a patient with a large hepatocellular carcinoma (HCC) (maximum diameter, 75 mm) in the right lobe. A-C: Sonographic angiograms acquired by CE 3D US with the Static 3D in the early phase and rendered using the maximum intensity projection mode alone, presented in different directions, showing the tumor containing the tortuous intratumoral vessels.

7. Characterization of liver lesions by CE 3D US with Sonazoid

Sonazoid-enhanced 3D US also provides important spatial visualization of any part of the VOI. From the early to the late phase, Sonazoid-enhanced 3D US shows tumor vascularity and changes in tumor enhancement patterns in multiplanar images. In our retrospective study of 139 liver lesions, the diagnostic accuracies of Sonazoid-enhanced 3D US and contrast-enhanced 3D CT were assessed for differentiating among liver lesions. The sensitivity of both modalities was 83% or higher, the specificity was 87% or higher for Sonazoid-enhanced 3D US and 92% or higher for contrast-enhanced 3D CT, the positive predictive value was 71% or higher for both modalities, and the area under the receiver operating characteristics curve (A_z) was 0.89 or more for US and 0.92 or more for CT. The inter-reader agreement was good to excellent ($\kappa \geq 0.76$) for both modalities (Luo et al., 2009c).

8. Features of hypervascular HCCs on CE 3D US with Sonazoid

Typical hypervascular HCCs contain intratumoral vessels and show tumor enhancement in the early phase, show homogeneous or heterogeneous tumor enhancement (slight washout) in the middle phase, and become hypoechoic, showing a distinct boundary with the surrounding liver parenchyma (washout) in the late phase (Figs. 4-6). Most moderately and poorly differentiated HCCs show these enhancement patterns, whereas about half of the hypervascular well-differentiated HCCs appear as isoechogenic areas in the late phase. It must be borne in mind that about half of the hypervascular well-differentiated HCCs are not detected as perfusion defects in the late phase of Sonazoid-enhanced US.

The main rendering mode used for obtaining sonographic angiograms in the early phase for hypervascular HCCs is the maximum intensity projection mode, mixed with some other mode at a different percentage, which enables depiction of the tumor staining and tumor vessels in three dimensions at any visual angles desired. Sonographic angiograms also demonstrate the relationship between the reconstructed tumor staining and the surrounding vessels (Figs. 4C, 5A). The main rendering mode used for obtaining sonographic

angiograms in the late phase for typical hypervascular HCCs is the average intensity mode mixed with the surface mode at a different percentage, which enables depiction of the lesions as hypoechogenic (washout) areas.

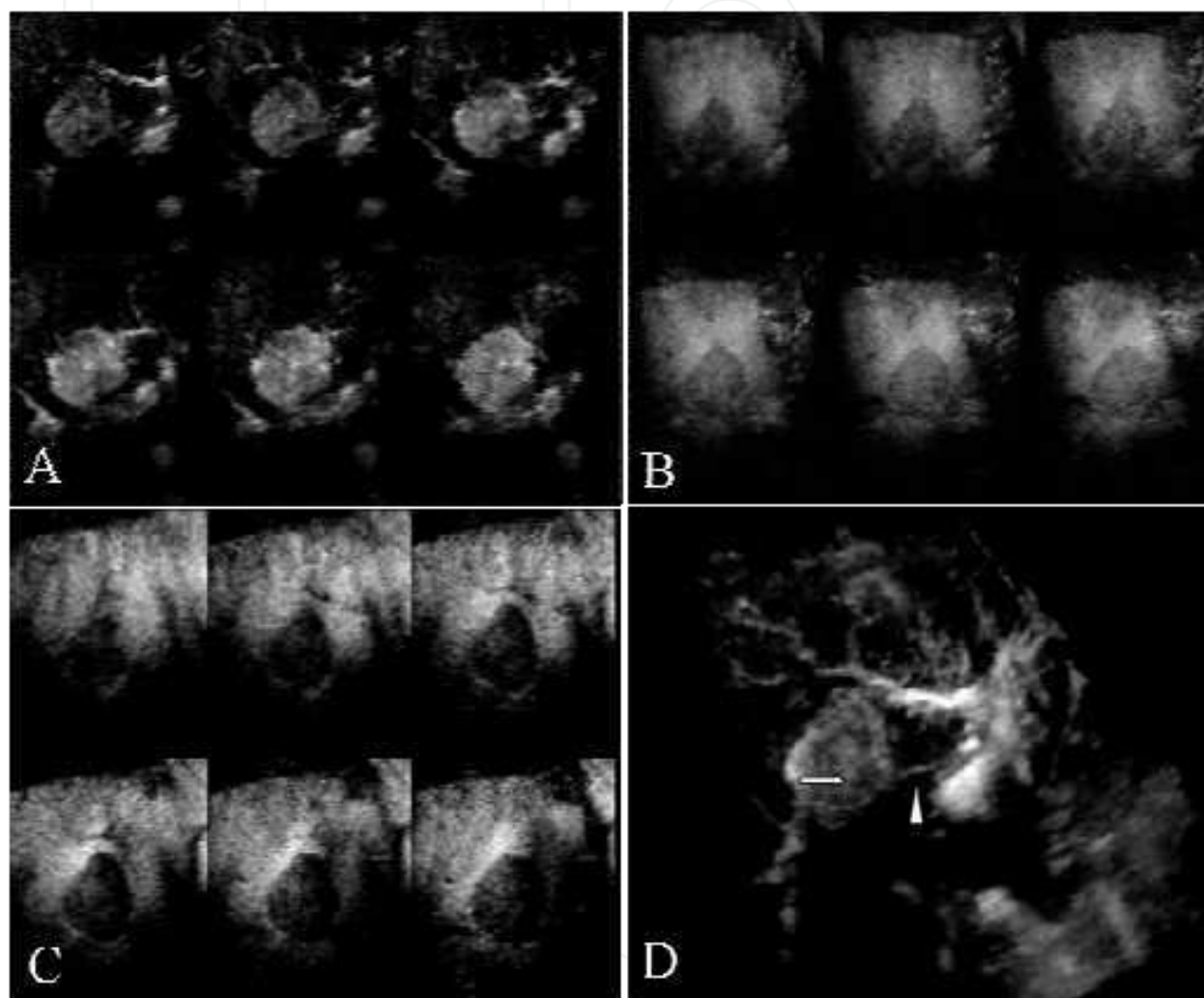


Fig. 4. CE 3D US images of the liver in a patient with HCC (maximum diameter, 40 mm) located adjacent to the left portal vein in segment IV of the left lobe. A-C: TUI in plane A of the early phase (A), middle phase (B), and late phase (C). The slice distance was 3.5 mm in each plane. These images show homogeneous tumor enhancement with intratumoral vessels in the early phase, homogeneous enhancement (slight washout) in the middle phase, and hypoechogenicity (washout) in the late phase. Sonographic angiograms acquired with the Autosweep 3D function in the early phase and rendered using the maximum intensity projection mode mixed with the surface mode showing the feeding artery (arrowhead) and homogeneous tumor enhancement with intratumoral vessels (arrow) (D). The left portal vein is also seen.

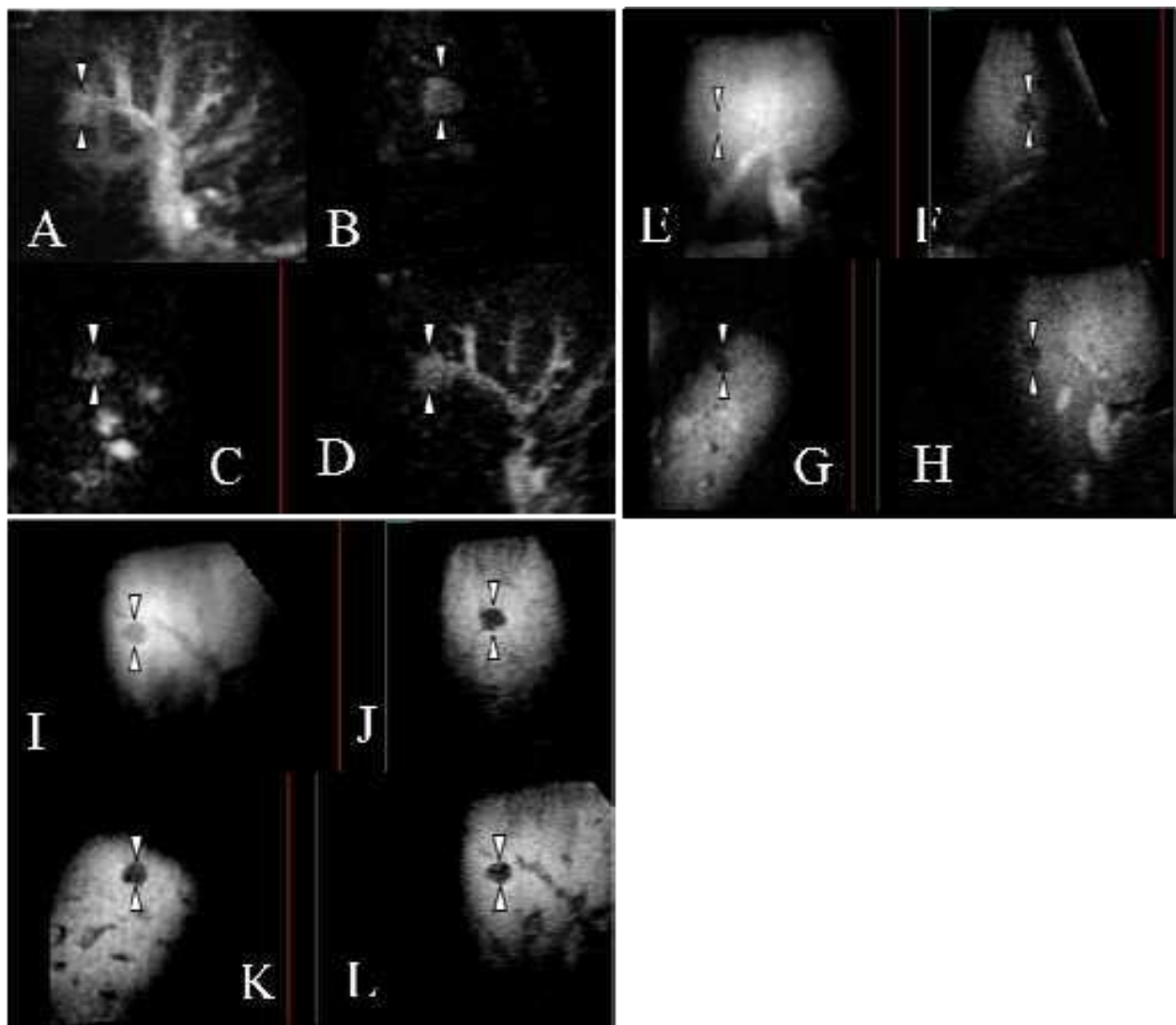


Fig. 5. CE 3D US images of the liver in a patient with a small HCC located adjacent to the right anterior portal vein (maximum diameter, 13 mm) in segment VIII of the right lobe. A-D: Display of a sonographic angiograms acquired with the Autosweep 3D function in the early phase and rendered using the maximum intensity projection mode mixed with the surface mode (A) and 3D plane B, which could be translated from right to left (B), plane C, which could be translated from bottom to top (C), plane A, which could be translated from front to back (D); these images show homogeneous enhancement of the tumor with intratumoral vessels adjacent to the portal vein and hepatic artery. E-H: Display of sonographic angiograms acquired with the Autosweep 3D function in the middle phase and rendered using the average intensity mode mixed with the surface mode (E) and 3D plane B (F), plane C (G), plane A (H); these images exhibit the lesions as perfusion defect. I-L: Display of sonographic angiograms acquired with the Autosweep 3D function in the late phase and rendered using the average intensity mode mixed with the surface mode (I) and 3D plane B (J), plane C (K), plane A (L); these images exhibit the lesion as a hypoechogenic (washout) area. Arrowheads indicate the margin of the tumor. Therefore, this HCC shows homogeneous enhancement with intratumoral vessels in the early phase, appears as a perfusion defect in the middle phase, and as a hypoechogenicity (washout) in the late phase of the CE 3D US.

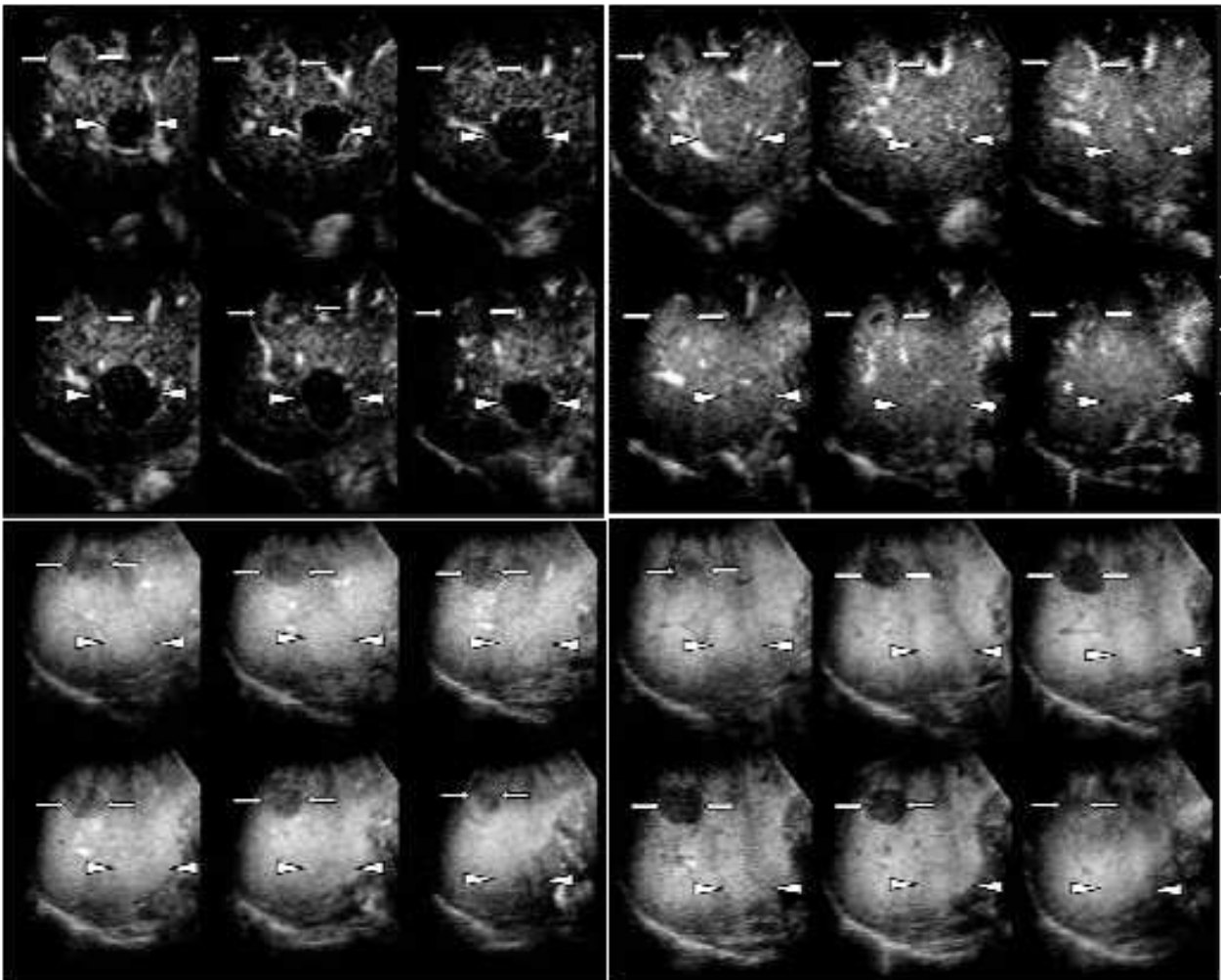


Fig. 6. CE 3D US images of the liver in a patient with a typical hypervascular HCC (maximum diameter, 20 mm) in segment VII (arrows) and a non-hypervascular (atypical) HCC (maximum diameter, 30 mm) in segment VI (arrowheads) in the right lobe. A-D: TUI in plane A obtained at 22 sec (A) and 37 sec (B) (the early phase), 1 min 45 sec (the middle phase) (C), and 6 min 45 sec (the late phase) after injection of Sonazoid (D). The slice distance was 4.4 mm in each plane. As for the HCC located in segment VII (arrows), the tumor shows heterogeneous enhancement with intratumoral vessels in the early phase (A, B), homogeneous enhancement (slight washout) in the middle phase (C), and appears as a hypoechogenic (washout) area in the late phase (D). This HCC was a moderately differentiated HCC. As for the HCC located in segment VI (arrowheads), these images show hypoechogenicity (A), followed by homogeneous tumor enhancement without intratumoral vessels (isoechogenicity) (B) in the early phase, homogeneous enhancement in the middle phase (isoechogenicity) (C), and isoechogenicity (persistence of enhancement) in the late phase (D). This HCC was a well-differentiated HCC.

9. Features of atypical HCCs on CE 3D US with Sonazoid

Most non-hypervascular well-differentiated HCCs (early HCC) are visualized as hypo- to isoechogenic areas without obvious tumor vessels in the early phase, show diffuse enhancement in the middle phase (isoechogenicity), and appear as isoechogenic (persistence

of enhancement) areas in the late phase. Figure 6 shows a TUI showing coexistence of typical hypervascular HCC and early HCC in the right lobe of the liver.

Figure 7 shows a nodule-in-nodule type of HCC. A TUI of this lesion shows heterogeneous enhancement with intratumoral vessels in the early phase, and heterogeneous enhancement in the middle phase. In the late-phase TUI, the lesion exhibits partial hypoechogenicity (washout), corresponding to the enhanced area in the early phase, and isoechogenicity (persistence of enhancement) in the remaining area. In general, isoechogenicity in the late phase suggests the diagnosis of well-differentiated HCC and hypoechogenicity in the late phase suggests moderately well-differentiated HCC.

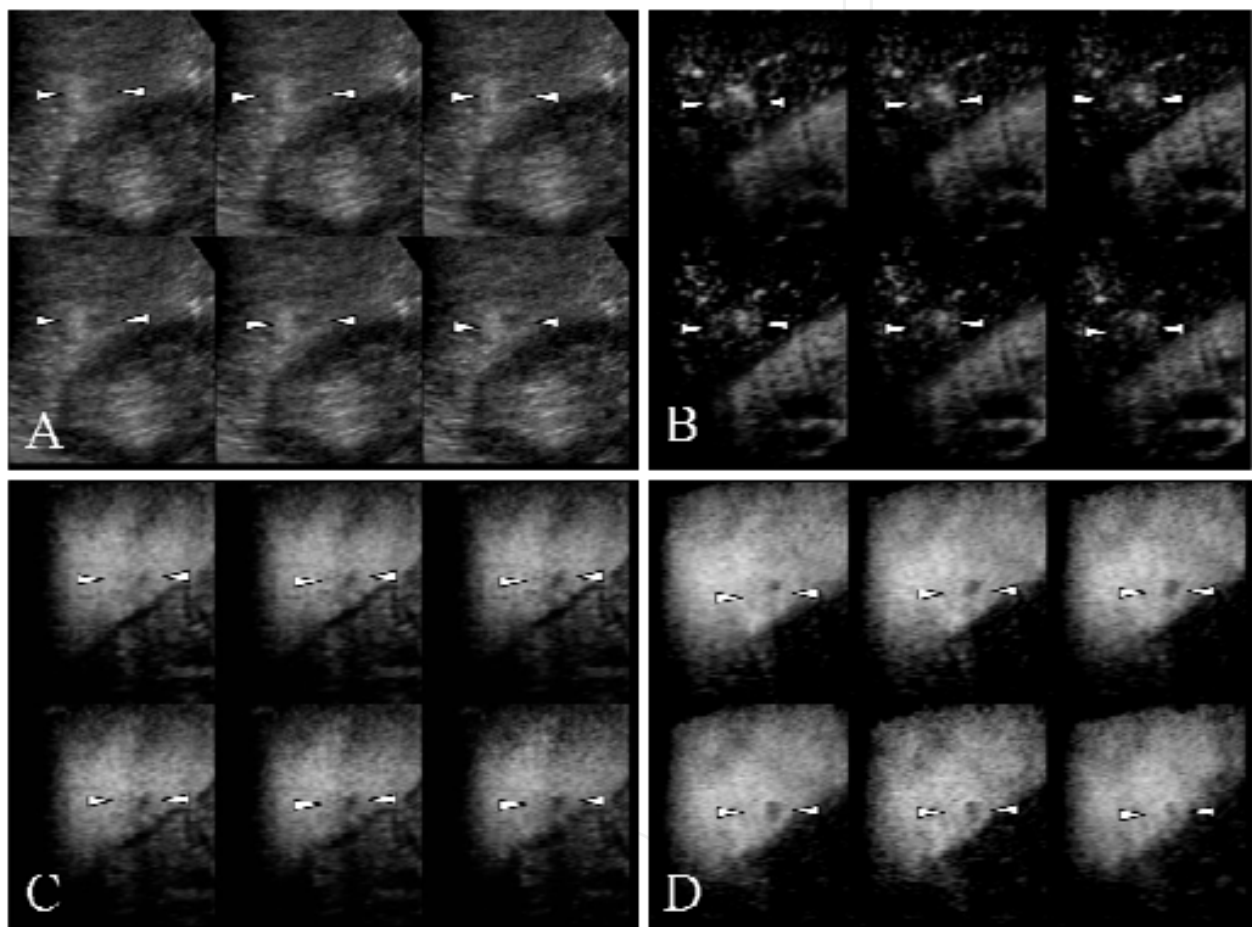


Fig. 7. 3D US and CE 3D US images of the liver in a patient with a nodule-in-nodule type of HCC (maximum diameter, 18 mm) in segment VI of the right lobe. A-D: TUI in plane A of B-mode, early phase (A), middle phase (B), and late phase (C). The slice distance was 0.5 mm in each plane. These images show the nodule-in-nodule lesion in the B-mode (A), heterogeneous enhancement with intratumoral vessels in the early phase (B), and heterogeneous enhancement in the middle phase (C). In the late-phase TUI, the lesion exhibits partial hypoechogenicity (washout), corresponding to the enhanced area in the early-phase image, and isoechogenicity (persistence of enhancement) in the remaining area (D), corresponding to the non-enhanced area in the early-phase image. Arrowheads indicate the margin of the tumor.

10. Features of hepatic metastases on CE 3D US with Sonazoid

The typical enhancement pattern of hepatic metastases consists of peripheral ring-like enhancement with peritumoral vessels (Fig. 8) or intratumoral vessels in the early phase, peripheral ring-like enhancement in the middle phase (wash out), and hypoechogenicity (wash out) in the late phase. As for hypervascular metastases, CE 3D US shows heterogeneous enhancement with intratumoral vessels in the early phase, peripheral ring-like enhancement (wash out) in the middle phase, and hypoechogenicity (wash out) in the late phase (Fig. 9). In this case, the enhancement pattern in the early phase was consistent with that of a hypervascular HCC. However, as compared to a hypervascular HCC, hypervascular metastases have a tendency to show an early washout pattern in the middle phase. This is a valuable finding for differentiating between these two tumors. Hypovascular hepatic metastases show peritumoral vessels without obvious enhancement in the early phase, appear as perfusion defects in the middle phase, and show hypoechogenicity (washout) in the late phase (Fig. 10).

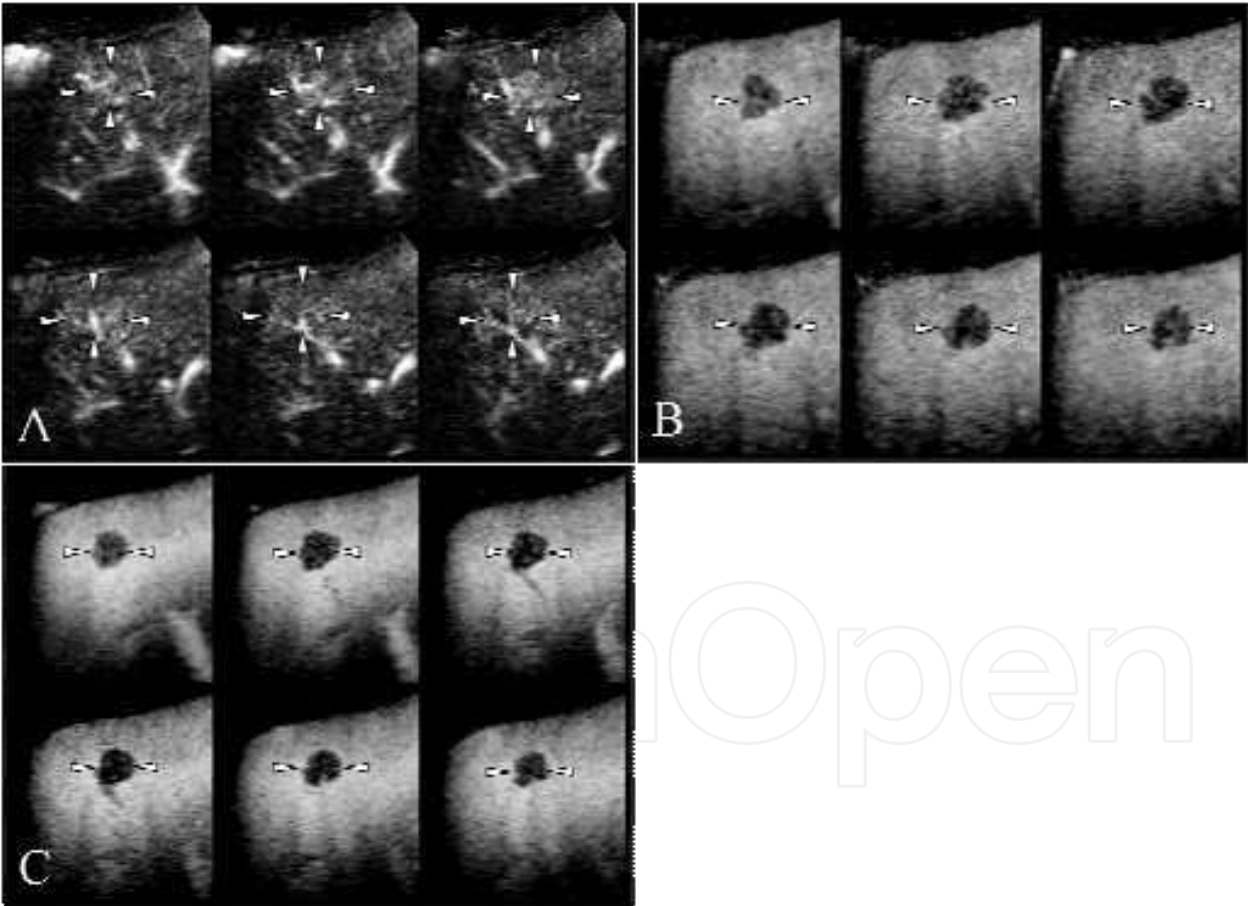


Fig. 8. CE 3D US images of the liver in a patient with metastasis from colon carcinoma (maximum diameter, 16 mm) in segment VIII of the right lobe. A-D: TUI in plane A of the early phase (A), middle phase (B), and late phase (C). The slice distance was 1.5 mm in each plane. These images show peripheral ring-like enhancement with peritumoral vessels in the early phase, peripheral ring-like enhancement in the middle phase (wash out), and hypoechogenicity (wash out) in the late phase. Arrowheads indicate the margin of the tumor.

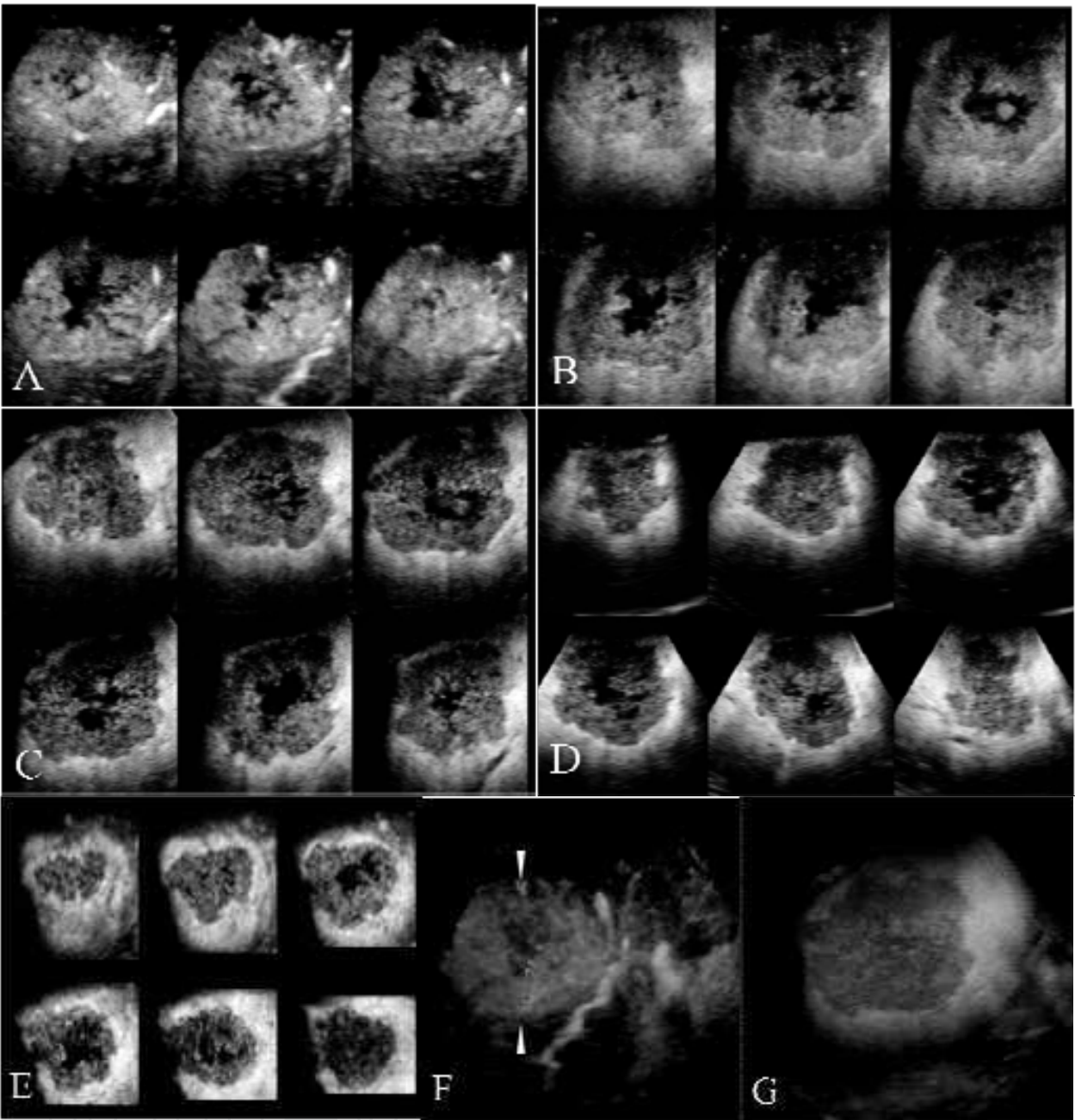


Fig. 9. CE 3D US images of the liver in a patient with metastasis from colon carcinoma (maximum diameter, 65 mm) in the right lobe. A-E: TUI in plane A with a slice distance of 5.4 mm of the early phase (A), middle phase (B), and late phase (C), in plane B with a slice distance of 8.2 mm (D) , and in plane C with a slice distance of 7.0 mm (E) of the late phase. These images show heterogeneous enhancement with intratumoral vessels in the early phase (A), peripheral ring-like enhancement (wash out) in the middle phase (B), and hypoechogenicity (wash out) in the late phase (C-E). A sonographic angiogram acquired with the Autosweep 3D function in the early phase and rendered using the maximum intensity projection mode mixed with the surface mode showing heterogeneous tumor enhancement with intratumoral vessels (arrow) adjacent to the hepatic artery (F). A sonographic angiogram acquired with the Autosweep 3D function in the late phase and rendered using the average intensity mode mixed with the surface mode showing the tumor as a hypoechogenicity (G).

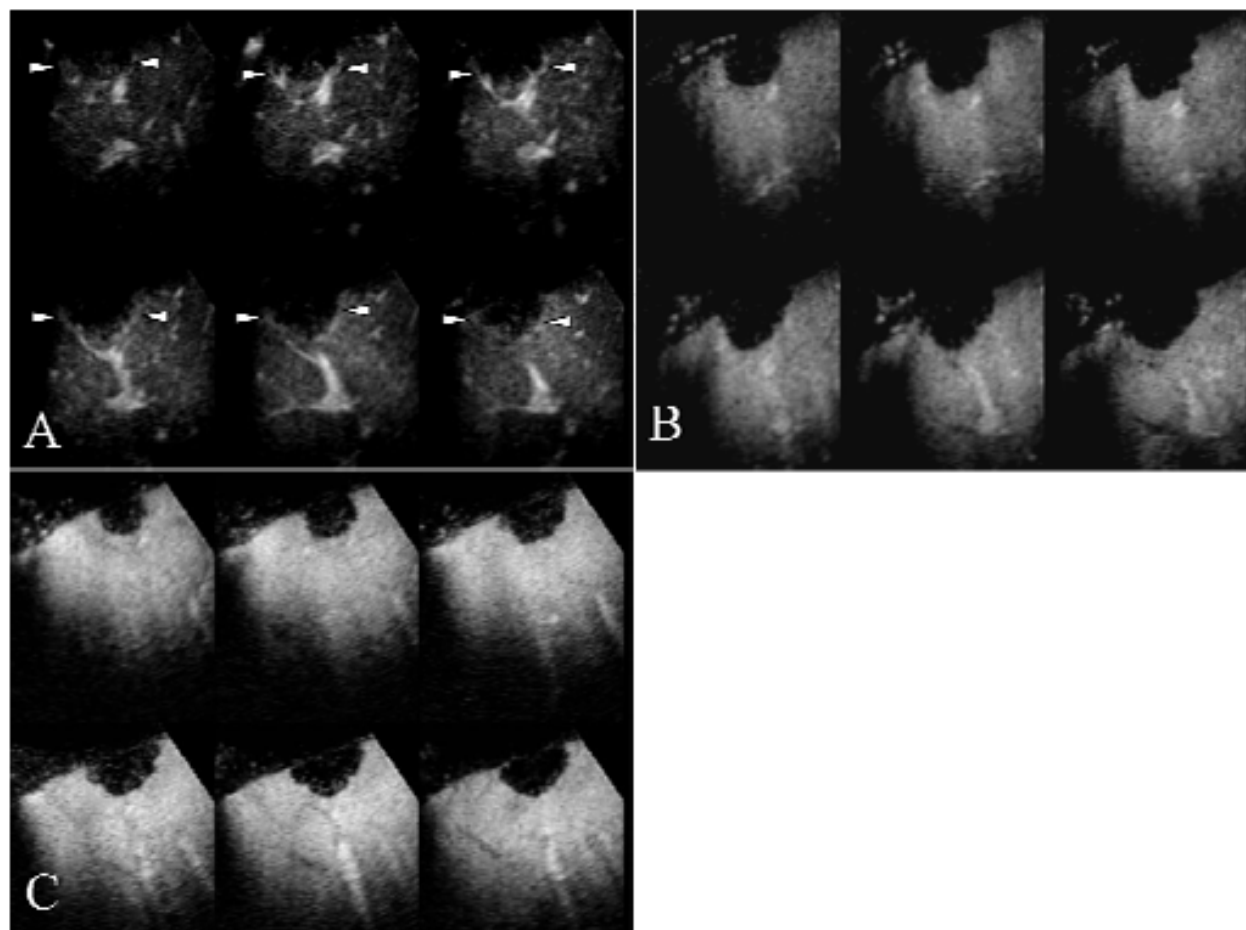


Fig. 10. CE 3D US images of the liver in a patient with metastasis from colon carcinoma (maximum diameter, 25 mm) in segment VIII in the right lobe. A-C: TUI in plane A of the early phase (A), middle phase (B), and late phase (C). The slice distance was 1.8 mm in each plane. These images show peritumoral vessels alone (arrows), without obvious enhancement in the early phase (A), perfusion defect in the middle phase (washout) (B), and hypoechogenicity (washout) in the late phase (C). Arrowheads indicate the margin of the tumor.

The main rendering mode used for obtaining sonographic angiograms in the middle and late phase for metastases is the average intensity mode, mixed with the surface mode at a different percentage, which enables depiction of the lesion as a hypoechogenic (washout) region. According to the vascularity in the early phase, we selected the main rendering mode for obtaining the sonographic angiograms. In cases with hypervascular metastases, the main rendering mode used is the maximum intensity projection mode, and in cases with lesions showing extensive unenhanced areas, we select the average intensity mode as the main rendering mode.

11. Features of hemangiomas on CE 3D US with Sonazoid

The typical enhancement pattern of a hepatic hemangioma consists of peripheral nodular enhancement without tumor vessels in the early phase, peripheral nodular enhancement in the middle phase, and isoechogenicity (persistence of enhancement) in the late phase (Fig. 11). Most hemangiomas appear as isoechogenicities or show incomplete fill-in and

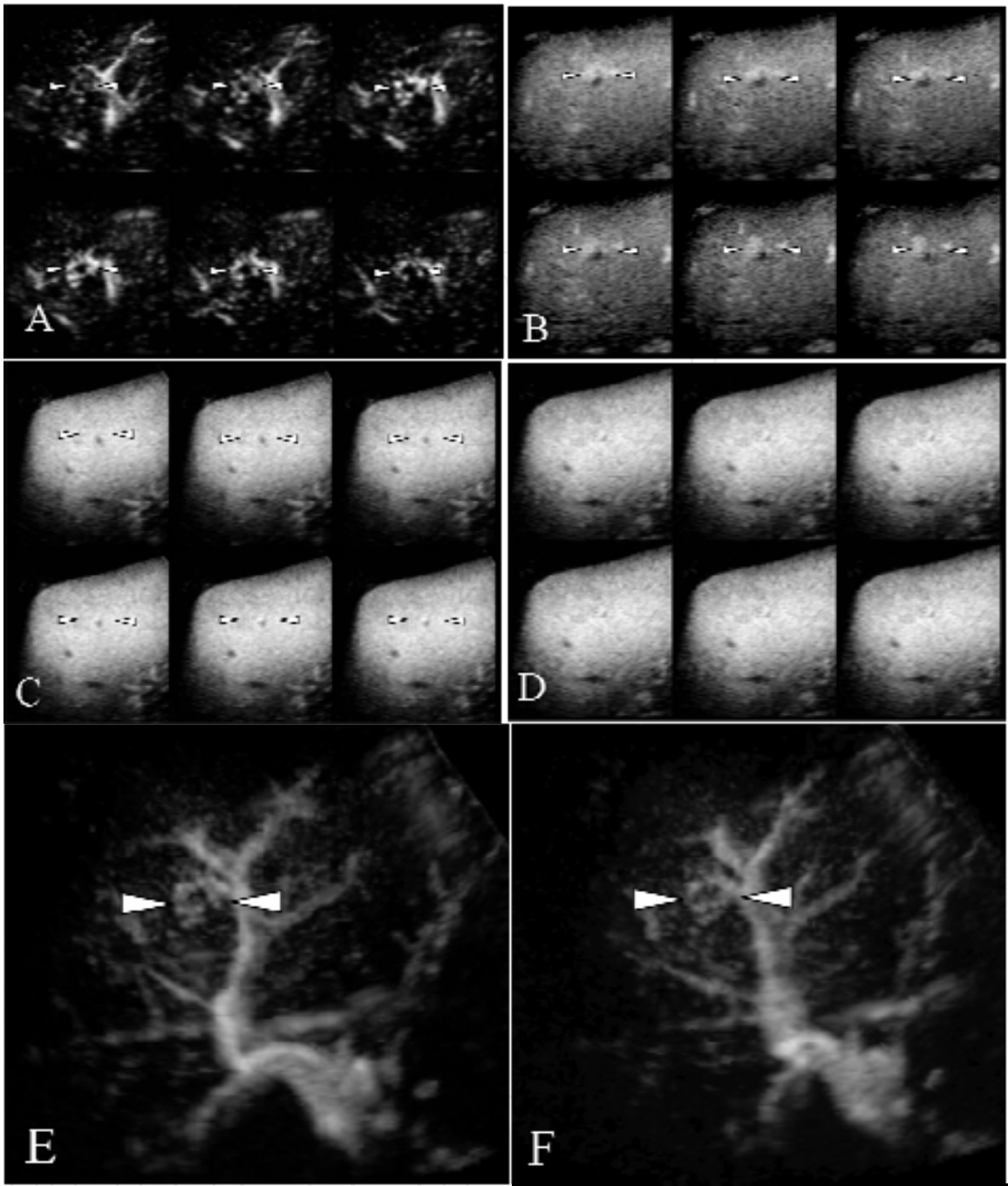


Fig. 11. CE 3D US images of the liver in a patient with a small hemangioma (maximum diameter, 13 mm) in segment VIII of the right lobe. A-D: TUI in plane A obtained at 21 sec (A) and 35 sec (B) (early phase), 1 min 30 sec (middle phase) (C), and 5 min 40 sec (late phase) after the injection of Sonazoid (D). A slice distance is 0.5 mm in each plane. These images show peripheral nodular enhancement without tumor vessels in the early phase (A, B), heterogeneous enhancement in the middle phase (C), and isoechogenicity (persistence of enhancement) in the late phase (D). Arrowheads indicate the margin of the tumor. A sonographic angiogram acquired with the Autosweep 3D function in the early phase and rendered using the average intensity mode mixed with the maximum intensity projection mode, presented in different directions, showing peripheral nodular enhancement without tumor vessels adjacent to the portal vein and the hepatic artery (E, F).

persistence of enhancement in the late phase; however, it must be borne in mind that in some cases, these tumors exhibit slight hypoechogenicity (slight washout) in the late phase (Fig.12). The enhancement pattern of high-flow type hemangiomas consists of homogeneous enhancement immediately after the peripheral nodular enhancement without tumor vessels in the early phase, homogeneous enhancement in the middle phase, and isoechogenicity (persistence of enhancement) in the late phase. Detection of peripheral nodular enhancement without tumor vessels in the early phase is very significant for the diagnosis of hemangioma.

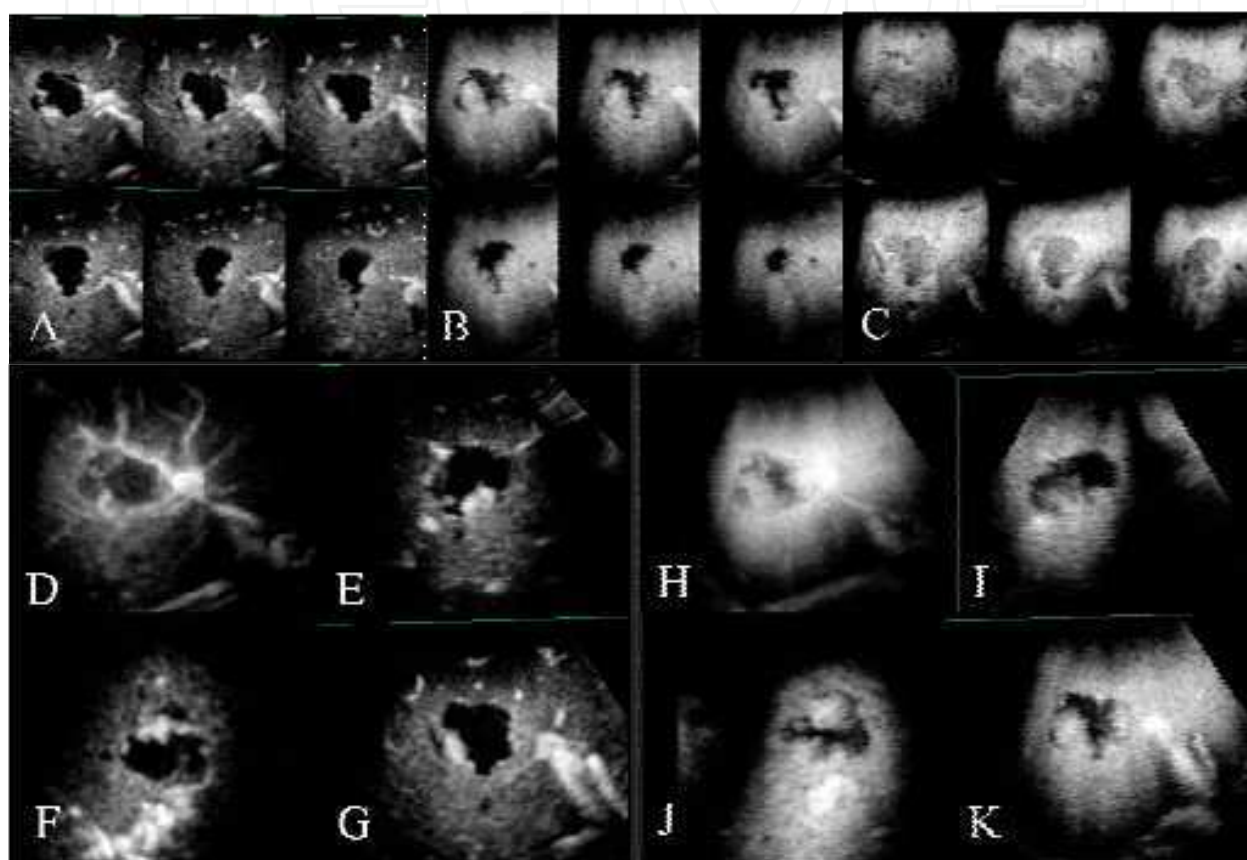


Fig. 12. CE 3D US images of the liver of a patient with hemangioma (maximum diameter, 35 mm) in segment VIII of the right lobe. A-C: TUI in plane A of the early phase (A), middle phase (B), and late phase (C). The slice distance was 3.5 mm in each plane. These images show peripheral nodular enhancement without tumor vessels in the early phase (A), peripheral nodular enhancement in the middle phase (B), and slight hypoechogenicity (slight washout) in the late phase (C). D-G: Display of a sonographic angiogram acquired with the Autosweep 3D function in the early phase and rendered using the average intensity mode mixed with the maximum intensity projection mode (D) and 3D plane B (E), plane C (F), plane A (G). These images show peripheral nodular enhancement without tumor vessels adjacent to the portal vein and the hepatic artery. H-K: Display of a sonographic angiogram acquired with the Autosweep 3D function in the middle phase and rendered using the average intensity mode mixed with the surface mode (H) and 3D plane B (I), plane C (J), plane A (K). These images exhibit the lesions as peripheral nodular enhancement.

The main rendering mode used for obtaining sonographic angiograms in every phase for hemangiomas is the average intensity mode, mixed with some other mode at a different percentage, which enables depiction of the unenhanced areas of the lesion as a hypoechogenic region.

12. Evaluation of the therapeutic efficacy of ablation therapy by CE 3D US with Sonazoid

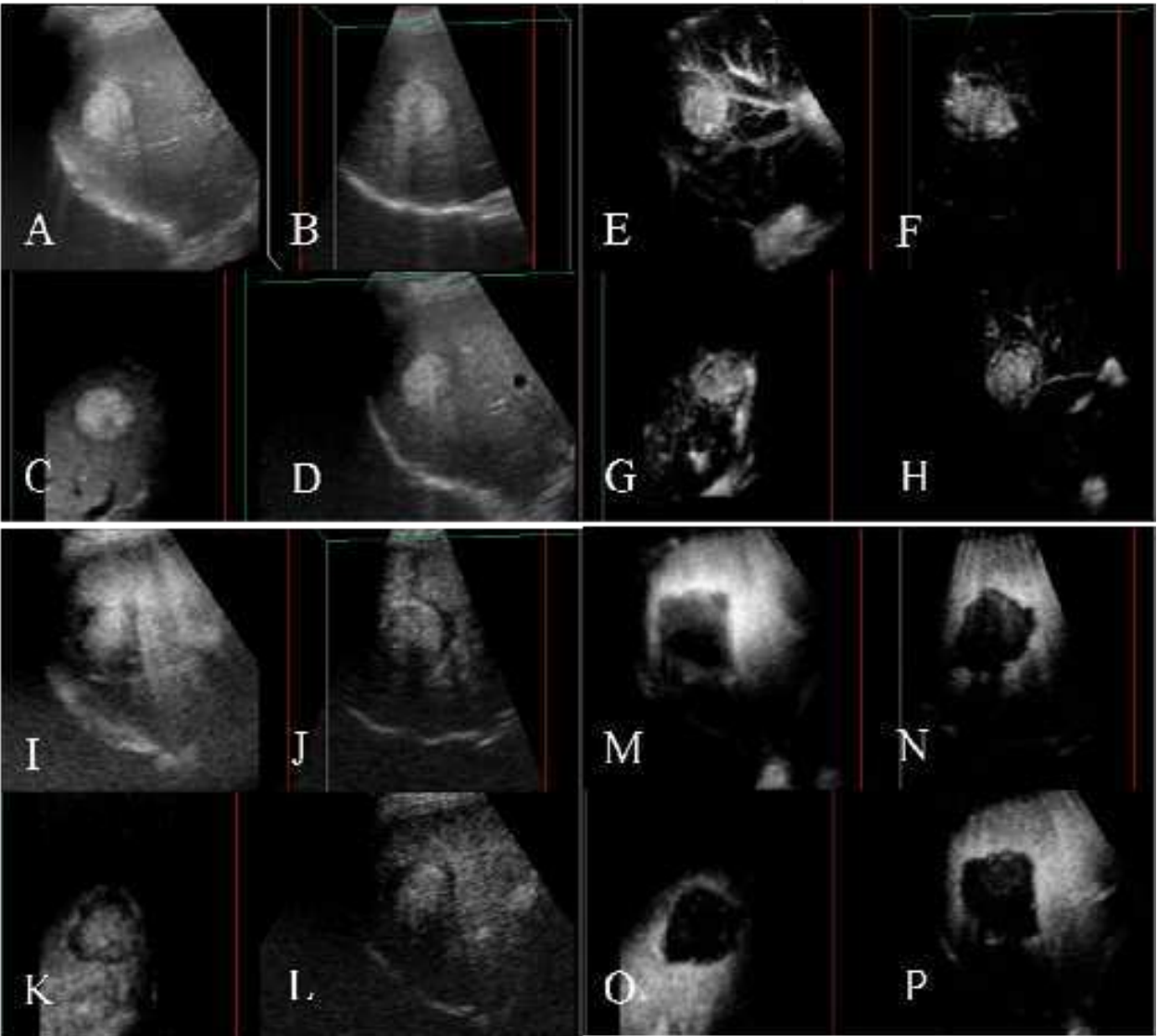


Fig. 13. 3D US and CE 3D US images of the liver in a patient with HCC located adjacent to the right anterior portal vein (maximum diameter, 29 mm), in segment VIII in the right lobe. A-D: Display of sonographic angiograms acquired with the Autosweep 3D function and

rendered using the surface mode (A) and 3D plane B, plane C (C), plane A (D) of the B-mode obtained before RFA showing a hyperechoic tumor.

E-H: Display of sonographic angiograms acquired with the Autosweep 3D function and rendered using the maximum intensity projection mode with the surface mode (E) and 3D plane B (F), plane C (G), plane A (H) of the early-phase images obtained before RFA showing homogeneous enhancement of the tumor with intratumoral vessels.

I-L: Display of sonographic angiograms acquired with the Autosweep 3D function and rendered using the average intensity with the surface mode (I) and 3D plane B (J), plane C (K), plane A (L) of the middle-phase CE 3D US using the CPI mode with a low mechanical index obtained 1 day after RFA showing the tumor itself and the ablated areas. However, the background B-mode appears to interfere with the clear visualization of sufficiently ablated areas.

M-P: Display of a sonographic angiograms acquired with the Autosweep 3D function and rendered using the average intensity with the surface mode (M) and 3D plane B (N), plane C (O), plane A (P) of the middle-phase CE 3D US using the CHA mode with a high mechanical index, which eliminates the background B-mode, obtained 1 day after RFA showing the necrotic areas as clear perfusion defects. This 3D view shows that the ablated area is slightly larger than the original tumor and that the safety of the margin is not sufficient; thus, the patient needed to be monitored closely for tumor recurrence; 22 months after the RFA, local recurrence was detected by dynamic MRI.

CE 3D US imaging with Sonazoid allows 3D visualization for comparison with a high sensitivity of HCC tumors before treatment with the treated areas after ablation. Use of the CHA mode and a high mechanical index eliminates the background B-mode and emphasizes the microbubbles in the vessels, allowing residual tumors to be differentiated from necrotic areas after ablation. Using this method, we recently demonstrated the usefulness of automatically scanned CE 3D US with Sonazoid for early evaluation of the therapeutic efficacy of percutaneous RFA for HCC lesions (Fig. 13) (Luo et al., 2010b).

Sonazoid-enhanced 3D US can also be used to evaluate the immediate therapeutic effects of high-intensity focused ultrasound (HIFU) on small HCC lesions. This modality has the potential to allow detection of residual HCCs after such treatment, thereby enabling additional HIFU ablation to be performed for residual untreated portions (Numata et al., 2010b).

13. Side effects of Sonazoid

Sonazoid is associated with a low incidence of side effects, such as diarrhea 1.6%, albuminuria 1.6%, and neutropenia 1.0%. It is not contraindicated for patients with renal dysfunction or iodine allergy, although one reported contraindication for Sonazoid in patients is a history of egg allergy (Moriyasu & Itoh, 2009).

14. Limitations

First, CE 3D US of focal liver lesions has the shortcoming of potentially including artifacts from the heart and respiratory movements (Figs. 2B, C), rib cage, and interference from

abdominal gas, etc. We attempted to minimize the influence of artifacts by requesting the patients to hold their breath during the scanning procedure, selecting the location of the volume transducer, mediating the size and position of the VOI, adjusting the scanning angle, and reconstructing the sonographic angiogram using appropriate rendering modes. Second, when multiple lesions were detected in one VOI, we could scan the lesions simultaneously in the early phase; however, when multiple lesions were located in separate VOI, only one VOI could be evaluated by CE 3D US in the early phase. Third, until recently, Sonazoid was only available in Japan, which might the spread of CE 3D US using this contrast agent.

15. Conclusions

CE 3D US, which is convenient to perform and does not involve radiation exposure, appears to be promising as a novel and useful method for three-dimensional evaluation of the vascular characteristics of liver tumors and for the differential diagnosis of hepatic lesions with good diagnostic capability. These features of CE 3D US are anticipated to be of benefit in the clinical setting. This modality can also be potentially useful for evaluating the effects of RF ablation or HIFU for HCCs, offering unique 3D visualization. We hope that in the near future, a fusion imaging method that would allow fusion and synchronization of CE 3D US images with multiplanar reconstruction CT or MR images on a single screen in real-time will become available in the near future.

16. References

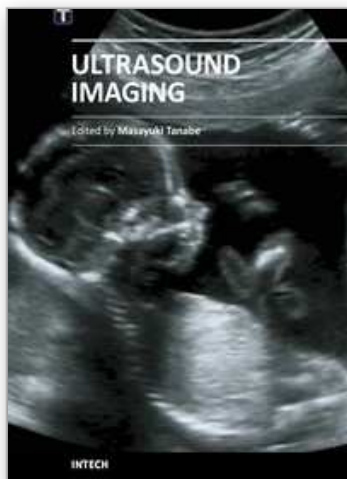
- Badea R, Socaciu M, Lupşor M, et al. (2007). Evaluating the liver tumors using three-dimensional ultrasonography: A pictorial essay. *JGastrointestin Liver Dis*, 16, 1, 85-92.
- Benacerraf BR, Shipp TD, Bromley B. (2006). Three-dimensional US of the fetus: volume imaging. *Radiology*, 238, 2, 988-996.
- Bosch FX, Ribes J, Díaz M, et al. (2004). Primary liver cancer: worldwide incidence and trends. *Gastroenterology*, 127, S51, S5-S16.
- Camaggi V, Piscaglia F, Bolondi L. (2007). Recent advances in the imaging of hepatocellular carcinoma. From ultrasound to positron emission tomography scan. *Saudi Med J* 28, 7, 1007-1014.
- Dietrich CF. (2002). 3D real time contrast enhanced ultrasonography, a new technique. *Rofo*, 174, 2, 160-163.
- Forsberg F, Goldberg BB, Merritt CR, et al. (2004). Diagnosing breast lesions with contrast-enhanced 3-dimensional power Doppler imaging. *JUltrasound Med*, 23, 2, 173-182.
- Halpern EJ, McCue PA, Aksnes AK, et al. (2002). Contrast-enhanced US of the prostate with Sonazoid: comparison with whole-mount prostatectomy specimens in 12 patients. *Radiology*, 222, 2, 361-366.
- Kotsianos-Hermle D, Wirth S, Fischer T, et al. (2009). First clinical use of a standardized three-dimensional ultrasound for breast imaging, *Eur J Radiol*, 71, 1, 102-108.

- Krenning BJ, Kirschbaum SW, Soliman OI et al. (2007). Comparison of contrast agent-enhanced versus non-contrast agent-enhanced real-time three-dimensional echocardiography for analysis of left ventricular systolic function. *Am J Cardiol*, 100, 9, 1485-1489.
- Kudo M. (2007). New sonographic techniques for the diagnosis and treatment of hepatocellular carcinoma. *Hepatol Res*, 37, S2, S193-S199.
- Luo W, Numata K, Morimoto M, et al. (2009a). Clinical utility of contrast-enhanced three-dimensional ultrasound imaging with Sonazoid: findings on hepatocellular carcinoma lesions. *Eur J Radiol*, 72, 3, 425-431.
- Luo W, Numata K, Morimoto M, et al. (2009b). Three-dimensional contrast-enhanced sonography of vascular patterns of focal liver tumors: pilot study of visualization methods. *AJR Am J Roentgenol*, 192, 1, 165-173.
- Luo W, Numata K, Morimoto M, et al. (2009c). Focal liver tumors: characterization with 3D perflubutane microbubble contrast agent-enhanced US versus 3D contrast-enhanced multidetector CT. *Radiology*, 251, 1, 287-295.
- Luo W, Numata K, Morimoto M, et al. (2010a). Differentiation of focal liver lesions using three-dimensional ultrasonography: retrospective and prospective studies. *World J Gastroenterol*, 16, 17, 2109-2119.
- Luo W, Numata K, Morimoto M, et al. (2010b). Role of Sonazoid-enhanced three-dimensional ultrasonography in the evaluation of percutaneous radiofrequency ablation of hepatocellular carcinoma. *Eur J Radiol*, 75, 1, 91-97.
- Moriyasu F and Itoh K. (2009). Efficacy of perflubutane microbubble-enhanced ultrasound in the characterization and detection of focal liver lesions: phase 3 multicenter clinical trial. *AJR Am. J Roentgenol*, 193, 1, 86-95.
- Numata K, Morimoto M, Ogura T, et al. (2008). Ablation therapy guided by contrast-enhanced sonography with Sonazoid for hepatocellular carcinoma lesions not detected by conventional sonography. *J Ultrasound Med*, 27, 3, 395-406.
- Numata K, Luo W, Morimoto M, et al. (2010a). Contrast-enhanced ultrasound of hepatocellular carcinoma. *World J Radiol*. 28, 2, 68-82.
- Numata K, Fukuda H, Ohto M, et al. (2010b). Evaluation of the therapeutic efficacy of high-intensity focused ultrasound ablation of hepatocellular carcinoma by three-dimensional sonography with a perflubutane-based contrast agent. *Eur J Radiol*, 75, 2, e67-e75.
- Ohto M, Kato H, Tsujii H, Maruyama H, et al. (2005) Vascular flow patterns of hepatic tumors in contrast-enhanced 3-dimensional fusion ultrasonography using plane shift and opacity control modes. *J Ultrasound Med*, 24, 1, 49-57.
- Taylor LS, Rubens DJ, Porter BC, et al. (2005). Prostate cancer: three-dimensional sonoelastography for in vitro detection. *Radiology*, 237, 3, 981-985.
- Tutschek B, Sahn DJ. (2007). Three-dimensional echocardiography for studies of the fetal heart: present status and future perspectives. *Cardiol Clin*, 25, 2, 341-355.
- Wessels T, Bozzato A, Mull M, et al. (2004). Intracranial collateral pathways assessed by contrast-enhanced three-dimensional transcranial color-coded sonography. *Ultrasound Med Biol*, 30, 11, 1435-1440.

Yukisawa S, Ohto M, Masuya Y et al. (2007). Contrast-enhanced three-dimensional fusion sonography of small liver metastases with pathologic correlation. *JClin Ultrasound*, 35, 1, 1-8.

IntechOpen

IntechOpen



Ultrasound Imaging

Edited by Mr Masayuki Tanabe

ISBN 978-953-307-239-5

Hard cover, 210 pages

Publisher InTech

Published online 11, April, 2011

Published in print edition April, 2011

In this book, we present a dozen state of the art developments for ultrasound imaging, for example, hardware implementation, transducer, beamforming, signal processing, measurement of elasticity and diagnosis. The editors would like to thank all the chapter authors, who focused on the publication of this book.

How to reference

In order to correctly reference this scholarly work, feel free to copy and paste the following:

Kazushi Numata, Wen Luo, Manabu Morimoto, Hiroyuki Fukuda, Naoto Sato and Katsuaki Tanaka (2011). Clinical Usefulness of Contrast-Enhanced Three-Dimensional Ultrasound Imaging with Sonazoid for Hepatic Tumor Lesions, Ultrasound Imaging, Mr Masayuki Tanabe (Ed.), ISBN: 978-953-307-239-5, InTech, Available from: <http://www.intechopen.com/books/ultrasound-imaging/clinical-usefulness-of-contrast-enhanced-three-dimensional-ultrasound-imaging-with-sonazoid-for-hepa>

INTech
open science | open minds

InTech Europe

University Campus STeP Ri
Slavka Krautzeka 83/A
51000 Rijeka, Croatia
Phone: +385 (51) 770 447
Fax: +385 (51) 686 166
www.intechopen.com

InTech China

Unit 405, Office Block, Hotel Equatorial Shanghai
No.65, Yan An Road (West), Shanghai, 200040, China
中国上海市延安西路65号上海国际贵都大饭店办公楼405单元
Phone: +86-21-62489820
Fax: +86-21-62489821

© 2011 The Author(s). Licensee IntechOpen. This chapter is distributed under the terms of the [Creative Commons Attribution-NonCommercial-ShareAlike-3.0 License](https://creativecommons.org/licenses/by-nc-sa/3.0/), which permits use, distribution and reproduction for non-commercial purposes, provided the original is properly cited and derivative works building on this content are distributed under the same license.

IntechOpen

IntechOpen